Binding energies of impurity states in strained wurtzite GaN/$Al_xGa_{1-x}N$ heterojunctions with finitely thick potential barriers*

Feng Zhen-Yu(冯振宇)†, Ban Shi-Liang(班士良)‡, and Zhu Jun(朱 俊)

College of Physical Science and Technology, Inner Mongolia University, Hohhot 010021, *China*

(Received 23 August 2013; revised manuscript received 28 December 2013; published online 10 April 2014)

Ground state binding energies of donor impurities in a strained wurtzite GaN/$Al_xGa_{1-x}N$ heterojunction with a potential barrier of finite thickness are investigated using a variational approach combined with a numerical computation. The built-in electric field due to the spontaneous and piezoelectric polarization, the strain modification due to the lattice mismatch near the interfaces, and the effects of ternary mixed crystals are all taken into account. It is found that the binding energies by using numerical wave functions are obviously greater than those by using variational wave functions when impurities are located in the channel near the interface of a heterojunction. Nevertheless, the binding energies using the former functions are obviously less than using the later functions when impurities are located in the channel far from an interface. The difference between our numerical method and the previous variational method is huge, showing that the former should be adopted in further work for the relevant problems. The binding energies each as a function of hydrostatic pressure are also calculated. But the change is unobvious in comparison with that obtained by the variational method.

Keywords: wurtzite, GaN/$Al_xGa_{1-x}N$ heterojunction, impurity state, binding energy

PACS: 68.35.bg, 68.47.Fg, 74.78.Fk **DOI:** 10.1088/1674-1056/23/6/066801

1. Introduction

In recent years, the physical properties of wurtzite AlGaN/GaN heterostructures have been widely studied due to their promising applications in devices such as the heterostructure field-effect transistor with high electron mobility, laser device with high frequency, etc.[1–5] A great number of experimental and theoretical studies indicate that there exists a strong built-in electric field (BEF) in nitride heterostructure due to the spontaneous and strain-induced piezoelectric polarization[6–9] since the lattice mismatch between AlN and GaN and their large piezoelectric coefficients. Bernardini *et al.*[10,11] studied *ab initio* the spontaneous polarization and piezoelectric constants of the III–V nitrides AlN, GaN, and InN. It was found that the piezoelectric constants are up to ten times larger than those in conventional III–V and II–VI semiconductor compounds. Using a similar approach, Wagner and Bechstedt[12] studied the structural, dielectric, lattice-dynamical, and electronic properties of biaxially and uniaxially strained group-III nitrides. Sánchez-Rojas *et al.*[13] presented the internal electric field distributions in $Al_xGa_{1-x}N$/GaN and $In_xGa_{1-x}N$/GaN heterostructures grown on (0001) GaN. Fonoberov *et al.*[14–16] theoretically investigated exciton states in strained GaN/AlN quantum dots to show the modification of the strain field. In addition, the same group[17,18] expanded their discussion on exciton states in ZnO quantum dots. Pokatilova *et al.*[19] studied acoustic phonon spectra and group velocities in AlN/GaN/AlN with an ultra-thin layer of wurtzite GaN. Later, Pokatilova *et al.*[20–22] investigated the effects of the BEF and strain on the electron mobility in AlN/GaN/AlN heterostructure. Saidi *et al.*[23] theoretically investigated the electron transport in delta-doped AlGaN/GaN heterostructure and found that the AlGaN/GaN heterostructures with higher Al compositions are favorable for higher electron densities. Gökden *et al.*[24,25] studied the scattering properties of the donors in systems of this kind and found that electron mobility is ultimately limited by optical phonon scattering at high temperatures and the dislocation scattering prevails at low temperatures. At intermediate temperatures, acoustic deformation potential and piezoelectric scattering are dominant and the lifetime ratio is larger for dislocation scattering than for impurity scattering. Wan *et al.*[26] studied the valence band offset (VBO) of an $Al_{0.17}Ga_{0.83}N$/GaN heterojunction by X-ray photoelectron spectroscopy and found that the heterojunction exhibits a type-I band alignment. Shen *et al.*[27] investigated the electrical and optical properties of InGaN/AlGaN double heterostructure blue light-emitting diodes and observed that the dominant mechanism of carrier transport across the junction is associated with carrier tunneling. Wen *et al.*[28] studied the influence of polarization effects on the energy band of AlGaN/GaN/AlGaN heterostructures and found that there exist

*Project supported by the National Natural Science Foundation of China (Grant No. 60966001) and the Key Project of the Natural Science Foundation of Inner Mongolia Autonomous Region, China (Grant Nos. 20080404Zd02 and 2013ZD02).

†Corresponding author. E-mail: xiaofzhenyu@163.com

‡E-mail: slban@imu.edu.cn

© 2014 Chinese Physical Society and IOP Publishing Ltd

two-dimensional electron gas (2DEG) and hole well at the heterointerfaces. These investigations are helpful to discuss the relevant physical properties in strained wurtzite heterostructures.

In early years, Ban and Hasbun[29,30] studied the ground state of an electron bound to a donor impurity near a single heterointerface by considering the influence of a realistic heterojunction potential and the screened Coulombic impurity potential. Later on, Kasapolgu *et al.*[31] studied the binding energies of shallow donor impurities in different shaped quantum wells (QWs) with an applied electric field. Recently, Zhang and Ban[32,33] adopted a variational method to investigate the Stark effect on shallow impurity states near the interface in a free-standing wurtzite GaN/$Al_xGa_{1-x}N$ heterojunction including the strain modification on material parameters. Xia *et al.*[34] studied variationally the ground-state donor binding energy in zinc-blende GaN/AlGaN asymmetric coupled QWs under hydrostatic pressure. The result showed that the donor binding energy is highly dependent on impurity position, structure parameters, and hydrostatic pressure. It should be pointed out that the previous authors almost assumed the barriers of QWs or heterojunctions to be infinite. However, a more practical situation for devices is that the barriers are finite thick.[35–37] For example, the structure of a GaN/$Al_xGa_{1-x}N$ heterojunction is that a GaN buffer layer was first formed on a sapphire substrate and then a finite-thick $Al_xGa_{1-x}N$ layer and a layer of GaN, which can be assumed to be infinite, were grown.

To demonstrate the finite barrier effect for impurity states in a GaN/$Al_xGa_{1-x}N$ heterojunction, in the paper we deal with the binding energies of impurity states using a numerical computation[38] to obtain wave functions of a bound electron in the z direction. Furthermore, it is shown that our numerical computation has a big improvement in the accuracy of the result compared with the variational method.[39] The influcence of the electron image potential was found to be negligibly small and can be excluded.[40]

The remainder of this paper is organized as follows. In Section 2, we describe the model and the calculation of a wurtzite GaN/$Al_xGa_{1-x}N$ realistic heterojunction. Then, the pressure and the strain coefficients of GaN and $Al_xGa_{1-x}N$ are discussed in Section 3. In Section 4, the numerical results are discussed. Finally, conclusions are drawn from the present study in Section 5.

2. Model and calculation

We consider a wurtzite GaN/$Al_xGa_{1-x}N$ realistic heterojunction with GaN layer, which can be assumed to be infinite, as the channel side, denoted by material 1 and located at $z > 0$. The $Al_xGa_{1-x}N$ barrier with a thickness of z_b is assumed to be finite (this is similar to the case of a real device), and is denoted by material 2 and located at $-z_b < z < 0$. For $z < -z_b$, the potential is a vaccum potential. The z axis is taken to be parallel to the c axis and the x–y plane parallel to the interface.

Within the framework of effective mass approximation, the Hamiltonian of a conduction electron bound to a donor impurity bearing a charge e located at $(0, 0, z_0)$ in the system is given as

$$H = H_z + H_{x-y} + H_c, \tag{1}$$

with

$$H_z = -\frac{\hbar^2}{2}\frac{\partial}{\partial z}\left[\frac{1}{m_e^{\perp}(z)}\right]\frac{\partial}{\partial z} + V(z) + eF_b z, \tag{2}$$

$$H_{x-y} = -\frac{\hbar^2}{2m_e^{\parallel}(z)}\frac{1}{\rho}\frac{\partial}{\partial\rho}\rho\frac{\partial}{\partial\rho}, \tag{3}$$

and

$$H_c = -\frac{e^2}{4\pi\kappa_0\kappa(z,z_0)\sqrt{\rho^2+(z-z_0)^2}}. \tag{4}$$

Here, $\rho = \sqrt{x^2+y^2}$ is the radial component of the electron coordinates in the x–y plane, $m_e^{\parallel}(z)$ and $m_e^{\perp}(z)$ are the values of effective mass of the electron parallel and perpendicular to the z direction respectively, which can be written as

$$m_e^{\beta}(z) = \begin{cases} m_{e,GaN}^{\beta}, & (z > 0), \\ x.m_{e,AlN}^{\beta} + (1-x).m_{e,GaN}^{\beta}, & (-z_b < z < 0). \end{cases}$$

Here, superscript β represents the orientation parallel or perpendicular to the z direction,. In Eq. (2), F_b is the BEF in the barrier and $V(z)$ is the barrier height. $\kappa(z,z_0)$ is the static dielectric constant related to the positions of the electron and the impurity, which can be given by

$$\kappa(z,z_0) = \begin{cases} \kappa_{01}, & z_0 > 0, z > 0, \\ \dfrac{\kappa_{01}+\kappa_{02}}{2}, & z_0 > 0, -z_b < z < 0. \end{cases}$$

According to the ratio of the conduction to the valance band offset,[39] the barrier height in Eq. (2) is determined by

$$V(z) = \begin{cases} 0, & z > 0, \\ 0.765(E_{g,b} - E_{g,w}), & -z_b \le z < 0. \end{cases} \tag{5}$$

The Schrödinger equation for a free electron in the z direction can be written as

$$H_z\varphi(z) = E_z\varphi(z). \tag{6}$$

The energy level E_z and wave function $\varphi(z)$ can be obtained by solving numerically Schrödinger Eq. (6) through using the finite difference method[38] (the obtained function is called the numerical wave function in the following) or by using a variational wave function.[39] By using the finite difference method, the eigenvalues converge to the minimum and the eigenvector and the eigenvalue can be obtained by using the iteration method until the difference between the present result and the previous result meets a certain accuracy. Equation (6) is chosen to obtain the corresponding wave function for an impurity

state interacted by a Coulombic potential for simplifying the calculation since the effects of barrier and triangular potential are dominant in influencing the wave function. Continuities of $\varphi(z)$ and $[1/m_e^{\perp}(z)][\mathrm{d}\varphi(z)/\mathrm{d}z]$ at interfaces are chosen as the boundary conditions in solving Eq. (6). For the condition $z < -z_b$, the wave function in the z direction is taken approximately to be zero since the potential is the vacuum potential, which is much larger than the barrier potential.

A one-parameter trial wave function in the x–y plane, which is used to calculate the variational energy of the impurity state, can be written as[29]

$$\phi(\rho) = \left(\frac{a}{2\pi}\right)^{1/2} \mathrm{e}^{-a\rho/2}, \tag{7}$$

where a is the variational parameter.

The variational energy of the ground state impurity can be expressed as

$$E(a) = \langle \psi(z,\rho)|H|\psi(z,\rho)\rangle, \tag{8}$$

where $\psi(z,\rho) = A\varphi(z)\phi(\rho)$ and A is the normalization constant.

Thus, the binding energy of the impurity ground state can be given by

$$E_b = E_{\mathrm{free}} - \min_a E(a), \tag{9}$$

where E_{free} is the ground state energy of the free electron, which can be obtained by repeating the above process but removing the Coulomb potential in Eq. (1) and replacing Eq. (8) by a plane wave function.

3. Pressure and strain coefficients

The uniaxial, biaxial strain and the modification of hydrostatic pressure on the electronic effective mass, dielectric constants, and the energy gap in GaN and $Al_xGa_{1-x}N$, can be taken into account in the following.

For heterojunctions with finite potential barriers, the biaxial lattice-mismatch induced strains are given as

$$\varepsilon_{xx,1} = \varepsilon_{yy,1} = \frac{a_{\mathrm{eq}}(p) - a_1(p)}{a_1(p)}, \tag{10}$$

and

$$\varepsilon_{xx,2} = \varepsilon_{yy,2} = \frac{a_{\mathrm{eq}}(p) - a_2(p)}{a_2(p)}, \tag{11}$$

where $a_\lambda(p)$ $(\lambda = 1,2)$ denotes the lattice constant of material λ under pressure p, $a_{\mathrm{eq}}(p)$ is the equilibrium lattice constant shared by all of the materials and can be written as[41]

$$a_{\mathrm{eq}}(p) = \frac{a_1(p)L_1 + a_2(p)L_2}{L_1 + L_2}, \tag{12}$$

in which L_λ is the width of material λ. For an infinite GaN-layer, i.e., $L_1 \to \infty$, $a_{\mathrm{eq}}(p) = a_1(p)$.

The pressure-dependent lattice constants $a_\lambda(p)$ can be given as[42]

$$a_\lambda(p) = a_\lambda(0)\left(1 - \frac{p}{3B_{0,\lambda}}\right), \quad (\lambda = 1,2), \tag{13}$$

where $B_{0,\lambda}$ is the material-dependent bulk modulus and can be expressed as

$$B_{0,\lambda} = \frac{[C_{11,\lambda} + C_{12,\lambda}]C_{33,\lambda} - 2C_{13,\lambda}^2}{C_{11,\lambda} + C_{12,\lambda} + 2C_{33,\lambda} - 4C_{13,\lambda}}, \quad (\lambda = 1,2). \tag{14}$$

From Hooke's law, the ratio between uniaxial and biaxial strain tensor can be given as[43]

$$\frac{\varepsilon_{zz,\lambda}}{\varepsilon_{xx,\lambda}} = \frac{C_{11,\lambda} + C_{12,\lambda} - 2C_{13,\lambda}}{C_{33,\lambda} - C_{13,\lambda}}, \quad (\lambda = 1,2). \tag{15}$$

Energy gaps each as a function of pressure and strain can be given as[44]

$$\begin{aligned} E_{\mathrm{g,GaN}}(p, \overleftrightarrow{\varepsilon}) &= E_{\mathrm{g,GaN}}(p) + 2(d_{1,\mathrm{GaN}} + b_{1,\mathrm{GaN}})\varepsilon_{xx,\mathrm{GaN}} \\ &\quad + (d_{2,\mathrm{GaN}} + b_{2,\mathrm{GaN}})\varepsilon_{zz,\mathrm{GaN}}, \end{aligned} \tag{16}$$

and

$$\begin{aligned} E_{g,\mathrm{AlN}}(p, \overleftrightarrow{\varepsilon}) &= E_{g,\mathrm{AlN}}(p) + 2d_{1,\mathrm{AlN}}\varepsilon_{xx,\mathrm{AlN}} \\ &\quad + d_{2,\mathrm{AlN}}\varepsilon_{zz,\mathrm{AlN}}, \end{aligned} \tag{17}$$

where $d_{1,\lambda}$, $d_{2,\lambda}$, $b_{1,\lambda}$, $b_{2,\lambda}$ are the deformation potentials in material λ. The corresponding energy gap of a ternary mixed crystal (TMC) $Al_xGa_{1-x}N$ can be determined by the simplified coherent potential approximation (SCPA) as[45]

$$E_{g,b} = \frac{E_A E_B}{xE_A + (1-x)E_B}, \tag{18}$$

where E_A and E_B are the energy gaps of GaN and AlN, respectively.

The pressure dependence of the electronic effective mass can be given by[46]

$$\frac{m_{0,\lambda}}{m_\lambda(p)} = 1 + \frac{C_\lambda}{E_{g,\lambda}(p)}, \quad (\lambda = 1,2), \tag{19}$$

where C_λ is a fixed value for a given material with $p = 0$.

The BEF is generated only in the finitely thick barrier-layer for the heterojunction and can be given as[47]

$$F_b = \frac{L_1(P_1^{\mathrm{pz}} + P_1^{\mathrm{sp}} - P_2^{\mathrm{pz}} - P_1^{\mathrm{sp}})}{L_2\varepsilon_{01} + L_1\varepsilon_{02}}, \tag{20}$$

where P_λ^{sp} is the spontaneous polarization, and P_λ^{pz} is the piezoelectric polarization and given as

$$P_\lambda^{\mathrm{pz}} = 2e_{31,\lambda}\varepsilon_{xx,\lambda} + e_{33,\lambda}\varepsilon_{zz,\lambda}. \tag{21}$$

Here, $e_{31,\lambda}$ and $e_{33,\lambda}$ are the piezoelectric constants, which can be given as[48]

$$e_{31,\lambda} = e_{31,\lambda}^{(0)} + \frac{4eZ_\lambda}{\sqrt{3}a_\lambda^2}\frac{\mathrm{d}u_\lambda}{\mathrm{d}\varepsilon_{xx,\lambda}}, \tag{22}$$

and

$$e_{33,\lambda} = e^{(0)}_{33,\lambda} + \frac{4eZ_\lambda}{\sqrt{3}a^2_\lambda}\frac{\mathrm{d}u_\lambda}{\mathrm{d}\varepsilon_{zz,\lambda}}. \tag{23}$$

The static dielectric constant is also influenced by the biaxial, uniaxial strain, and pressure. It can be derived from a generalized Lyddane–Sachs–Teller relation as

$$\kappa_{0,\alpha\alpha} = \kappa_{\infty,\alpha\alpha}\left(\frac{\omega_{\mathrm{LO},\alpha\alpha}}{\omega_{\mathrm{TO},\alpha\alpha}}\right)^2, \quad (\alpha = x,z), \tag{24}$$

where the frequencies of LO- and TO-phonons influenced by strain can be written as[43]

$$\omega_{\lambda,\alpha\alpha} = \omega_{\lambda,\alpha\alpha}(p) + 2K_{\lambda,xx}\varepsilon_{xx} + K_{\lambda,zz}\varepsilon_{zz}, \tag{25}$$

where $K_{\lambda,xx}$ and $K_{\lambda,zz}$ are the strain coefficients of phonon modes given in Ref. [47], and $\omega_{\lambda,\alpha\alpha}(p)$ can be given by[49]

$$\gamma_{\lambda,\alpha\alpha} = B_0\frac{1}{\omega_{\lambda,\alpha\alpha}}\frac{\partial\omega_{\lambda,\alpha\alpha}(p)}{\partial p}. \tag{26}$$

For the pressure dependence of high frequency dielectric constant, it is given by[50]

$$\frac{\partial\kappa_{\infty,\alpha\alpha}(p)}{\partial p} = -\frac{5(\kappa_{\infty,\alpha\alpha}-1)}{3B_0}(0.9 - f_{\mathrm{ion}}), \tag{27}$$

where f_{ion} is the ionicity of the material under pressure.

The dielectric constant of $Al_xGa_{1-x}N$ can be calculated by the SCPA as[45]

$$\kappa_{\mathrm{TMC}} = [((1-x)m_{\mathrm{AlN}}\kappa^2_{\mathrm{GaN}} + xm_{\mathrm{GaN}}\kappa^2_{\mathrm{AlN}})(x/m_{\mathrm{GaN}} + (1-x)/m_{\mathrm{AlN}})]^{1/2}. \tag{28}$$

4. Results and discussion

For convenience, the methods of using numerical wave functions and variational wave functions are denoted respectively by methods I and II in the following.

Wave functions of electrons as functions of position z for barrier thickness $z_b = 4$ nm for given impurity position $z_0 = 0$ are shown in Fig. 1. It indicates that the penetration into the barrier from the electron wave functions obtained by method I is more obvious than that by method II. Moreover, the penetration increases with z_b increasing at small values of z_b since the potential in the channel repulses the electrons to the barrier.

In a strained heterojunction, for a given Al concentration $x = 0.3$ and pressure $p = 0$, variations of binding energy E_b with impurity position z_0 for barrier thickness $z_b = 4$ nm are depicted in Fig. 2. It can be seen clearly that E_b obtained by method I is obviously greater than that by method II when impurity ions are located in the channel near the interface,

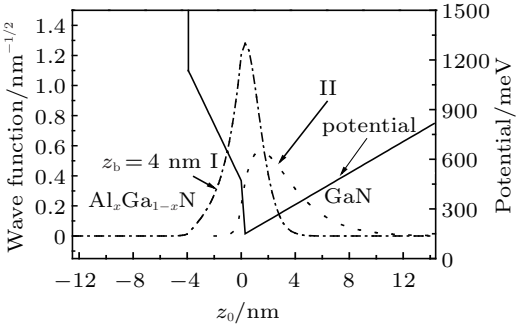


Fig. 1. Wave functions obtained by method I (dash–dotted line) and method II (dotted line) of electrons each as a function of position z for barrier thickness $z_b = 4$ nm with impurity ion position $z_0 = 0$. The potential (solid line) of the right axis represents the heterojunction potential barrier height between $Al_xGa_{1-x}N$ and GaN.

whereas the former is obviously less than the latter when impurity ions are located in the channel far from the interface. By using method I, the penetration of the electron can be considered sufficiently in comparison with that by using method II. When an impurity ion is located in the channel near the interface, E_b increases because of the enhancement of the Coulomb interaction induced by reducing the average distance between an electron and the impurity ion under the attraction of the BEF and the repulsion of the interface. Nevertheless, E_b decreases due to the weakened Coulomb interaction induced by increasing the average distance between an electron and the impurity ion when the impurity ion is located far from the interface since the repulsion of the interface and the attraction of the BEF become weaker as the impurity ion goes far from the interface.

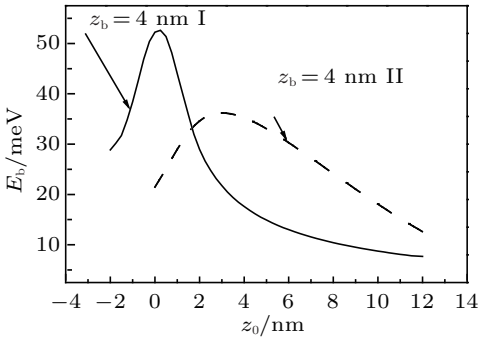


Fig. 2. Binding energy E_b as a function of impurity ion position for barrier thickness $z_b = 4$ nm when $x = 0.3$. Solid lines and dashed lines represent the results obtained by methods I and II, respectively.

Figure 3 shows values of E_b each as a function of z_b for different values of z_0 for $x = 0.3$. It can be seen that E_b decreases rapidly when the impurity ion moves from the interface to $z_0 = 4$ nm. When the impurity ion is located near the interface, E_b first reaches a maximum then decreases with z_b. This property is caused by the attraction of the BEF and the repulsion of the interface. The BEF plays a leading role when z_b is small. Otherwise, the repulsion of the interface plays a leading role when z_b is large.

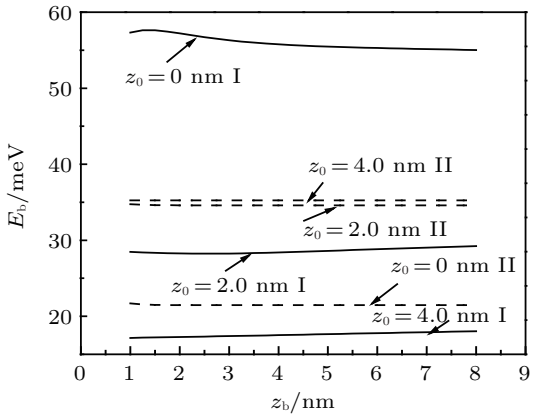


Fig. 3. Binding energies obtained by using methods I and II, each as a function of barrier thicknesses z_b for different values of impurity ion position z_0 when $x = 0.3$.

The values of E_b each as a function of pressure for different values of z_0 when $x = 0.3$ is given in Fig. 4. It can be seen that E_b increases almost linearly with hydrostatic pressure increasing, which is similar to the case of using method II. But the change is not obvious in comparison with using method II.

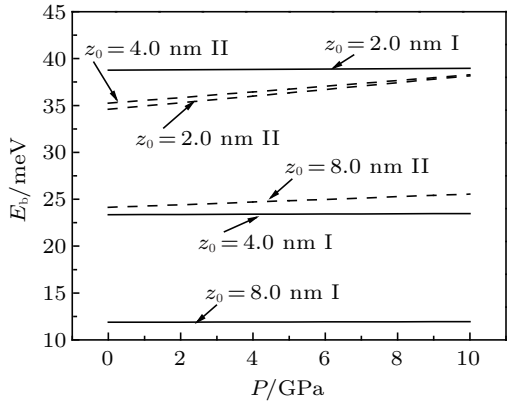


Fig. 4. Binding energies obtained by using methods I and II, each as a function of pressure for different values of impurity ion position z_0 with $z_b = 4$ nm when $x = 0.3$.

The values of E_b each as a function of x for different values of z_0 when $z_b = 4$ nm are shown in Fig. 5. When $z_0 = 4.0$ nm, E_b deceases with x increasing due to the comprehensive interaction between the repulsion of the interface and the Coulomb attraction to the electron. However, E_b deceases less obviously with x increasing when $z_0 = 8.0$ nm due to the weakened Coulomb interaction. It should be noted that the difference in E_b between using methods I and II increases with x increasing. When impurity ions are located in the channel near the interface, E_b obtained by method I is obviously greater than that by method II for a larger x. Nevertheless, the difference is less obvious when x is small. When an impurity ion is located in the channel near the interface, E_b deceases with x increasing by using method II due to the increasing repulsion of the interface. Furthermore, E_b deceases with x increasing less obviously by using method I due to the comprehensive interaction between the repulsion of the interface and the Coulomb attraction to the electron. Thus, method I is more suitable when the width of the barrier is small since the penetration of the electron can be considered sufficiently.

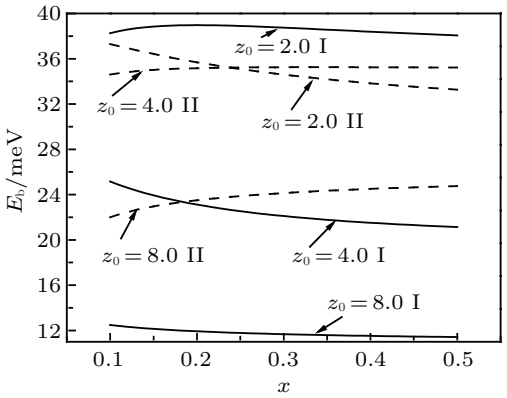


Fig. 5. Binding energies obtained by using method I, each as a function of Al component x for different values of impurity ion position z_0 when $z_b = 4$ nm.

5. Conclusion

We use a numerical computation method to calculate the ground state binding energies of donor impurities in a strained wurtzite GaN/$Al_xGa_{1-x}N$ heterojunction with a finitely thick potential barrier by taking into account the built-in electric field and the effects of ternary mixed crystals. The binding energies each as a function of the impurity ion position, the barrier width, Al component, and pressure, are discussed in detail and are compared with those using variational wave functions. The results show that the binding energies obtained using numerical wave functions are obviously greater than that using variational wave functions when impurities ions are located in the channel near the interface of a heterojunction. Nevertheless, the binding energies obtained using numerical wave functions are obviously less than those by using variational wave functions when impurity ions are located in the channel far from the interface. The binding energies increase almost linearly with pressure increasing, which is similar to those obtained using the variational wave functions but the change is less obvious. The difference between the binding energy obtained by using numerical wave functions and that by using the variational wave functions increases with Al content increasing.

References

[1] Miyoshi M, Ishikawa H, Egawa T, Asai K, Mouri M, Shibata T, Tanaka M and Oda O 2004 *Appl. Phys. Lett.* **85** 1710
[2] Kim T W, Choo D C, Yoo K H, Jung M H, Cho Y H, Lee J H and Lee J H 2005 *J. Appl. Phys.* **97** 103721
[3] Fu A B, Hao M R, Yang Y, Shen W Z and Liu H C 2013 *Chin. Phys. B* **22** 026803
[4] Sun Y F, Sun J D, Zhang X Y, Qin H, Zhang B S and Wu D M 2012 *Chin. Phys. B* **21**108504
[5] Ma X H, Pan C Y, Yang L Y, Yu H Y, Yang L, Quan S, Wang H, Zhang J C and Hao Y 2011 *Chin. Phys. B* **20** 027304

[6] Wu J Q 2009 *J. Appl. Phys.* **106** 011101
[7] Łepkowski S P, Teisseyre H, Suski T, Perlina P, Grandjean N and Massies J 2001 *Appl. Phys. Lett.* **79** 1483
[8] Łepkowski S P 2007 *Phys. Rev. B* **75** 195303
[9] Duan Y F, Li J B, Li S S and Xia J B 2008 *J. Appl. Phys.* **103** 023705
[10] Bernardini F, Fiorentini V and Vanderbilt D 1997 *Phys. Rev. B* **56** 10024
[11] Bernardini F, Fiorentini V and Vanderbilt D 2001 *Phys. Rev. B* **63** 193201
[12] Wagner J M and Bechstedt F 2002 *Phys. Rev. B* **66** 115202
[13] Sánchez-Rojas J L, Garrido J A and Muñoz E 2000 *Phys. Rev. B* **61** 2773
[14] Fonoberov V A and Balandin A A 2003 *J. Appl. Phys.* **94** 7178
[15] Fonoberov V A, Pokatilov E P and Balandin A A 2003 *J. Nanosci. Nanotechnol.* **3** 253
[16] Fonoberov V A 2004 *J. Vac. Sci. Technol. B* **22** 2190
[17] Fonoberov V A 2004 *Appl. Phys. Lett*. **85** 5971
[18] Fonoberov V A and Balandin A A 2004 *Phys. Rev. B* **70** 195410
[19] Pokatilova E P, Nika D L and Balandin A A 2003 *J. Superlattices and Microstructures* **33** 155
[20] Pokatilova E P, Nika D L, Askerov A S and Balandin A A 2007 *J. Appl. Phys.* **102** 054304
[21] Pokatilova E P 2006 *Appl. Phys. Lett.* **89** 113508
[22] Pokatilova E P, Nika D L and Balandin A A 2006 *Appl. Phys. Lett.* **89** 112110
[23] Saidi I, Bouzaiene L, Gazzah M H, Mejri H and Maaref H 2006 *Solid State Commun.* **140** 308
[24] Gökden S, I1gaz A, Balkan N and Mazzucato S 2004 *Physica E* **25** 86
[25] Gökden S 2004 *Physica E* **23** 19
[26] Wan X J, Wang X L, Xiao H L, Wang C M, Feng C, Deng Q W, Qu S Q, Zhang J W, Hou X, Cai S J and Feng Z H 2013 *Chin. Phys. Lett.* **30** 057101
[27] Shen B, Shi H T, Zhang R, Chen Z Z and Zheng Y D 2001 *Chin. Phys. Lett.* **18** 283
[28] Wen B, Jiang R L, Zhou J J, Ji X L, Liang L Y, Kong Y C, Shen B, Zhang R and Zheng Y D 2004 *Chin. Phys. Lett.* **21** 720
[29] Ban S L and Hasbun J E 1999 *Phys. Rev. B* **59** 2276
[30] Ban S L and Hasbun J E 1999 *Solid State Commun.* **109** 93
[31] Kasapolgu E, Sari H and Sokmen I 2003 *Physica B* **339** 17
[32] Zhang M and Ban S L 2009 *Chin. Phys. B* **18** 5437
[33] Zhang M and Ban S L 2009 *Chin. Phys. B* **18** 4449
[34] Xia C X, Zeng Z P and Wei S Y 2010 *Physica B* **405** 3237
[35] Yoshida S, Ishii H, Li J, Wang D L and Ichikawa M 2003 *Solid-State Electronics* **47** 589
[36] Wang Y, Ma L, Yu Z P and Tian L 2004 *Superlattices and Microstructures* **36** 869
[37] Tripathi N, Jindal V, Shahedipour-Sandvik F, Rajan S and Vert A 2010 *Solid-State Electronics* **54** 1291
[38] Zhu J, Ban S L and Ha S H 2012 *Mod. Phys. Lett. B* **26** 1250172
[39] Zhang M and Ban S L 2008 *Acta Phys. Sin.* **57** 4459 (in Chinese)
[40] Ban S L, Hasbun J E and Bull 1998 *Am. Phys. Soc*. **43** 914
[41] Kalliakos S, Lefebvre P and Taliercio T 2003 *Phys. Rev. B* **67** 205307
[42] Perlin P, Mattos L, Shapiro N A, Kruger J, Wong W S, Sands T, Cheung N W and Weber E R 1999 *J. Appl. Phys.* **85** 2385
[43] Wagner J M and Bechstedt F 2002 *Phys. Rev. B* **66** 115202
[44] Shan W, Hauenstein R J, Fischer A J, Song J J, Perry W G, Bremser M D, Davis R F and Goldenberg B 1996 *Phys. Rev. B* **54** 13460
[45] Ban S L and Hasbun J E 1999 *J. Eur. Phys. B* **8** 453
[46] Ting D Z Y and Chang Y C 1987 *Phys. Rev. B* **36** 4359
[47] Lepkowski S P, Teisseyre H, Suski T, Perlin P, Grandjean N and Massies J 1999 *Appl. Phys. Lett*. **79** 1483
[48] Vaschenko G, Patel D, Menoni C S, Gardner N F, Sun J, Götz W, Tomé C N and Clausen B 2001 *Phys. Rev. B* **64** 241308
[49] Petrov I, Mojab E, Powell R C, Greene J E, Hultman L and Sundgren J E 1992 *Appl. Phys. Lett.* **60** 2491
[50] Goñi A R, Syassen K and Cardona M 1990 *Phys. Rev. B* **41** 10104